Available online at www.sciencedirect.com
ScienceDirect
Acta Materialia 57 (2009) 2730–2738
Acta MATERIALIA
www.elsevier.com/locate/actamat

Formation mechanism of lamellar chips during machining of bulk metallic glass

M.Q. Jiang, L.H. Dai *

State Key Laboratory of Nonlinear Mechanics, Institute of Mechanics, Chinese Academy of Sciences, Beijing 100190, China

Received 27 November 2008; received in revised form 19 February 2009; accepted 19 February 2009
Available online 28 March 2009

Abstract

The unique lamellar chips formed in turning–machining of a Vit 1 bulk metallic glass (BMG) are found to be due to repeated shear-band formation in the primary shear zone (PSZ). A coupled thermomechanical orthogonal cutting model, taking into account force, free volume and energy balance in the PSZ, is developed to quantitatively characterize lamellar chip formation. Its onset criterion is revealed through a linear perturbation analysis. Lamellar chip formation is understood as a self-sustained limit-cycle phenomenon: there is autonomous feedback in stress, free volume and temperature in the PSZ. The underlying mechanism is the symmetry breaking of free volume flow and source, rather than thermal instability. These results are fundamentally useful for machining BMGs and even for understanding the physical nature of inhomogeneous flow in BMGs.

Keywords: Bulk metallic glass; Lamellar chip; Orthogonal cutting model; Free volume; Limit cycle

1. Introduction

Improved effectiveness has been a long-standing objective in metal machining and has often been achieved by increasing the cutting speed [1,2]. However, higher-speed cutting usually renders the chips formed imperfect-continuous, including chips with built-up edges [3], chips with periodic fractures [4], segmental chips [5], serrated chips [6], etc. The formation of these imperfect-continuous chips is often tied up with decreased tool life, degradation of the workpiece surface finish and less accuracy in the machined part [7,8]; hence, understanding the cause and effect of chip formation, which is nonlinear and dynamic in nature, is of practical importance. For conventional crystalline alloys, substantial process has been made in this respect over the past hundred years or so [1,9]. Bulk metallic glasses (BMGs) are a relatively young class of alloy materials which are envisaged to have a wide range functional and structural applications, exploiting their intriguing physical and mechanical properties [10–16]. In the course of practical applications, proper machining (cutting, drilling, grinding, etc.) with high effectiveness and precision is a necessary procedure [8,17–20]. However, explaining the deformation behavior and its underlying physics in BMG cutting processes lags well behind, and the mechanism of chip formation is central importance in this respect.

Previous works have shown that unique "continuous" chips with lamellar structure are prone to form during machining of BMGs, even at low cutting speeds [8,17,20]. Due to the low thermal conductivity of BMGs, it has been suggested that these lamellar chips are triggered by thermal instability resulting in periodically adiabatic shear bands (ASBs), just like serrated chip formation in crystalline metals [21]. In particular, this adiabatic shear localization-induced serrated chip can be mathematically explained as a bifurcation phenomenon: the limit cycle of the nonlinear dynamic system of tool–chip–workpiece during machining [22,23]. Because of their disordered atomic structure, BMGs have fundamentally different flow laws underpinned by discrete atomic jumps [24] or cooperative arrangements of local atomic clusters around the free volume site, termed

* Corresponding author. Tel.: +86 10 82543958; fax: +86 10 82543977.
E-mail address: lhdai@lnm.imech.ac.cn (L.H. Dai).

1359-6454/$36.00
doi:10.1016/j.actamat.2009.02.031

the "shear transformation zone" (STZ) [25] or "flow defect" [26]. Thus, the nonlinear evolution of free volume via STZs and its dynamic instability may be active in lamellar chip formation, though this has not yet been identified. Furthermore, does the limit-cycle bifurcation phenomenon still occur during the process of machining BMGs? What is its leading mechanism if the answer is affirmative? A detailed understanding of the chip morphology encountered in BMG machining is crucial not only for practical applications but also for understanding the nature of flow in these materials. In this paper, we develop a nonlinear dynamic model to quantitatively characterize lamellar chip formation in low-speed machining a $Zr_{41.2}Ti_{13.8}Cu_{10}Ni_{12.5}Be_{22.5}$ (Vit 1) BMG. The underlying physics of lamellar chip formation is clearly revealed.

2. Materials and methods

A typical BMG, Vit 1, was chosen for this study, because of its excellent glass-forming ability (GFA) [27,28], high thermal stability against crystallization and its potential as an advanced engineering material [29] in contrast to other systems. Master alloy ingots were produced by arc-melting the elements Zr, Ti, Cu, Ni and Be with a purity of 99.9% or better together under a Ti-gettered Ar atmosphere. To ensure homogeneity, the master alloy ingots were remelted several times and subsequently suction-drawn into copper molds to form rod-like BMG specimens 5 mm in diameter and 80 mm in length (Fig. 1 inset). The glassy nature was confirmed by X-ray diffraction (XRD) in a Philip PW 1050 diffractometer using Co $K\alpha$ radiation. As shown in Fig. 1, the BMG samples for machining tests showed only broad diffraction maxima and no peaks of crystalline phases were visible, revealing the amorphous structure. The turning–machining were conducted on a CK6150B computer-controlled lathe using a TiN-coated WC–Co insert (tool) with an invisible nose radius (<0.2 mm) and a $\alpha = 5°$ rake angle, as is illustrated in Fig. 2. All tests were done dry without using coolant, at 0.025 mm feed rev^{-1}, 0.1 mm depth of cut, and cutting speed 0.07 m s^{-1}. After machining, high-resolution scanning electron microscopy (HRSEM, FEI Sirion, spatial resolution 1.5 nm) was used to examine the chip morphology of all specimens.

3. Results

Fig. 3a displays one of the typical "continuous" twist chips formed during the machining of Vit 1 BMGs. The inset to Fig. 3a shows the macroscopic full-view of this chip. The tool–contact surface, marked by the arrow "A" in Fig. 3a, is presented in Fig. 3b. Although the surface looks macroscopically smooth, there are a large number of shear bands approximately perpendicular to the cutting direction. Fig. 3c is a high-magnification micrograph of an area, marked "C" in Fig. 3b. It can be clearly seen that the shear bands are nearly periodic with constant spacing on the micrometer scale. Their characteristic thickness is much thinner than that (~10–100 μm) of conventional ASBs in crystalline metals. Fig. 3d is the free surface of chip, as marked by the arrow "B" in Fig. 3a. A close-up view of the area "D" in Fig. 3d is displayed in Fig. 3e. Interestingly, a regular lamellar structure with a constant spacing of several micrometers (see Fig. 3f) clearly emerges, indicating the BMG chip is actually not perfectly continuous. Furthermore, no characteristic fracture patterns [30–32], such as vein-pattern, dimple, etc., were observed on both surfaces of this lamellar chip. This implies that the meniscus instability [33] or tension transformation zone (TTZ) [31] induced fracture does not take place during this chip formation. It is reasonable to believe that the chip lamella results from a periodic shear-banding formation, originating at the tool–contact surface (Fig. 3c) and propagating toward the free surface (Fig. 3d), in the so-called primary shear zone (PSZ) (as marked in Fig. 3f) [34]. From the viewpoint of phenomenology, lamellar chip formation during BMG machining is very similar to the formation of serrated chips in crystalline alloys, as shown in Fig. 4. Both of types of chip form via repeated inhomogeneous material

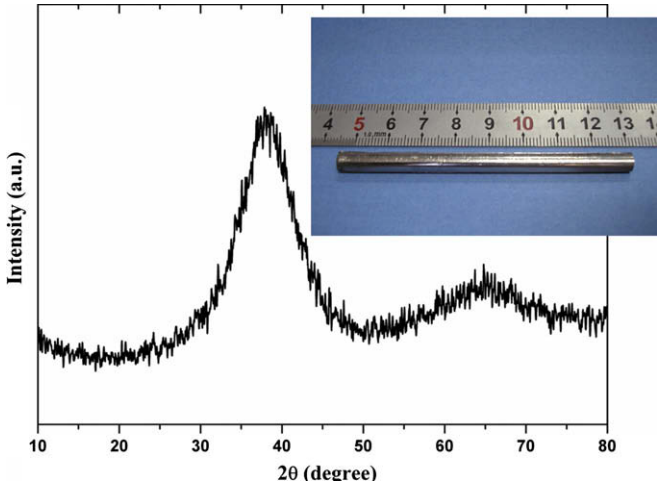

Fig. 1. XRD pattern of Vit 1 BMG rod.

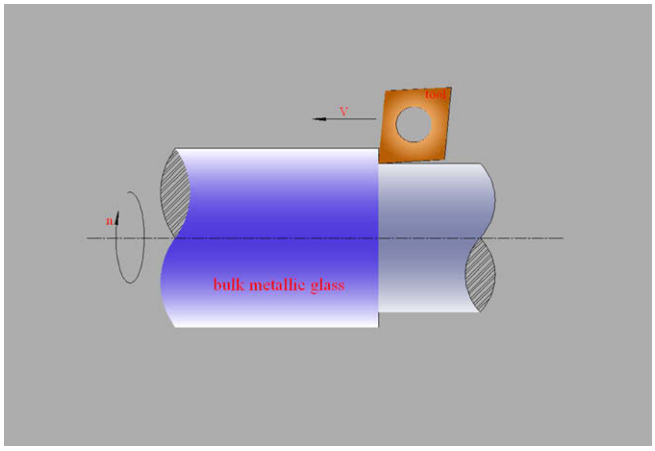

Fig. 2. Schematic for the lathe turning–machining of Vit 1 BMG.

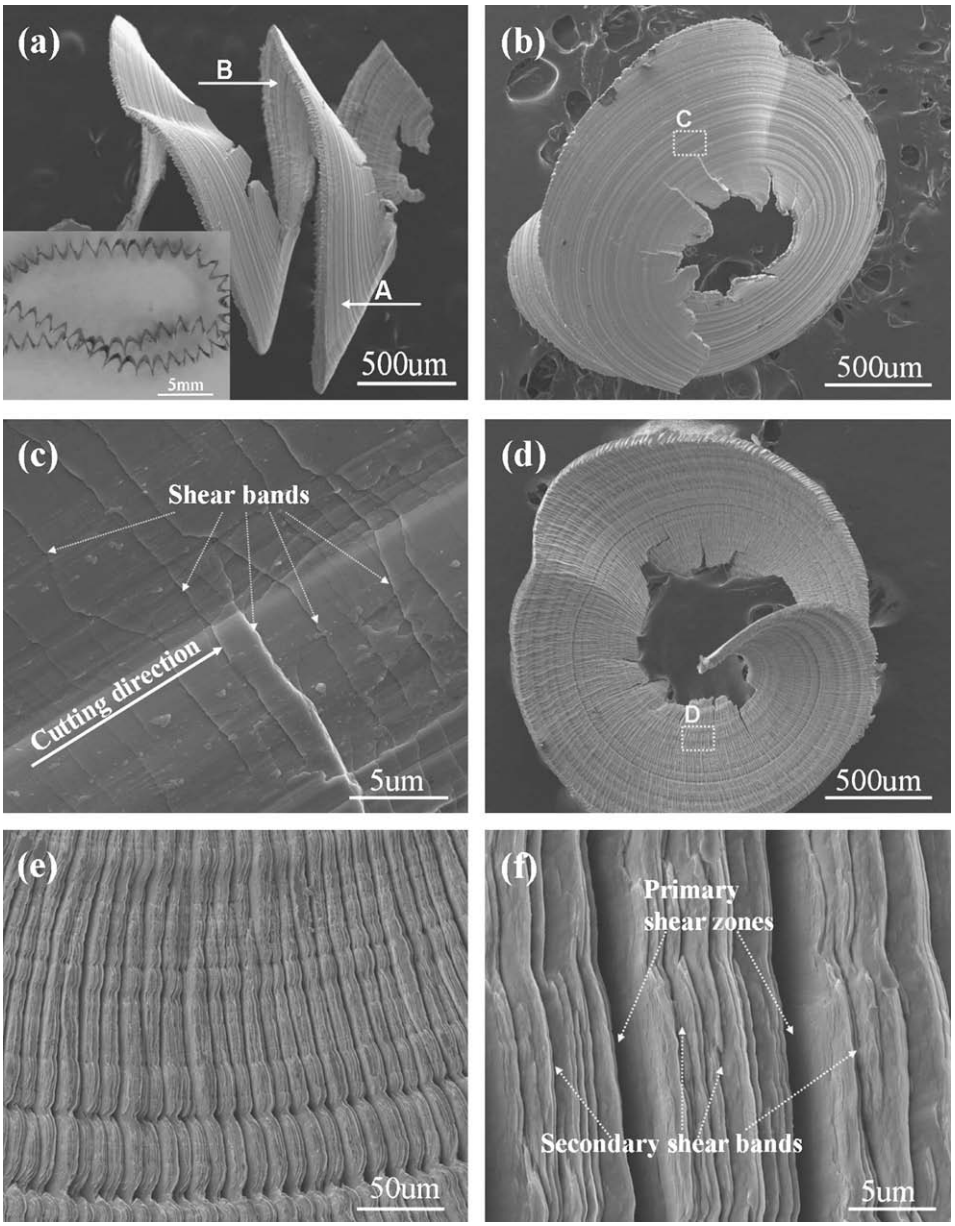

Fig. 3. Chip morphology of Vit 1 BMG. (a) Macroscopic full-view of the typical "continuous" twist chip. (b) Tool–contact surface of chip marked by "A" in (a). (c) Details corresponding to area "C" in (b). (d) Free surface of chip marked by "B" in (a). (e and f) lamellar structures at different magnifications in area "D" in (d).

flow (shear-band formation) in PSZs due to the interplay of tool and workpiece. However, several different features of lamellar chip morphology vis-à-vis that of serrated chip are evident by SEM observations (Fig. 3), summarized as follows: (i) the characteristic scales of shear bands and PSZs as well as their spacing δ_c (as marked in Fig. 4a) are much smaller; (ii) the free surface is relatively smooth or chip serration is weaker, implying a smaller shear displacement ψ (as marked in Fig. 4b) can result in shear-banding formation in BMGs; (iii) with the attendant primary shear bands in PSZs, many secondary shear bands (see Fig. 3f) between PSZs can be clearly observed on the free surface. These observations show that shear localization is likely to occur during machining a BMG, even at very low cutting speeds. An alternative mechanism for shear-banding instability and resultant lamellar chip formation in BMG cutting should exist. In fact, our previous theoretical analysis [35,36] indicates that the shear-banding instability is a coupled thermomechanical process dominated by local free-volume softening.

4. Theoretical modeling and discussion

4.1. Coupled thermomechanical orthogonal cutting model

The orthogonal machining model has successfully simulated continuous chip formation [34] and may be still valid for characterizing lamellar chips in BMGs. In fact, the

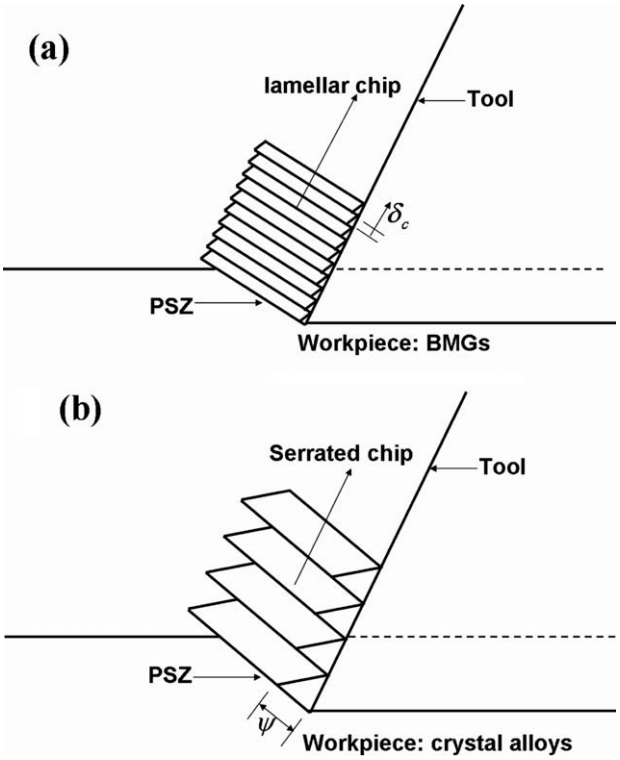

Fig. 4. Two-dimensional schematics of (a) lamellar chip formation in BMGs and (b) serrated chip formation in conventional crystalline alloys.

orthogonal cutting conditions are fulfilled to a good level of approximation for our present turning tests. Here, we consider a single-point machining (Fig. 5), in which the deformation of the material ahead of the tool occurs within the PSZ of infinitesimal thickness h. The PSZ extends from the tool–contact surface to the free surface, forming a shear angle ϕ with the surface generated. The Lagrangian coordinate Y is perpendicularly attached to the PSZ; $Y = 0$ lies on the lower plane of PSZ. Thus, the PSZ provides an indicator window to probe the nonlinear response of BMG to the tool's dynamic action.

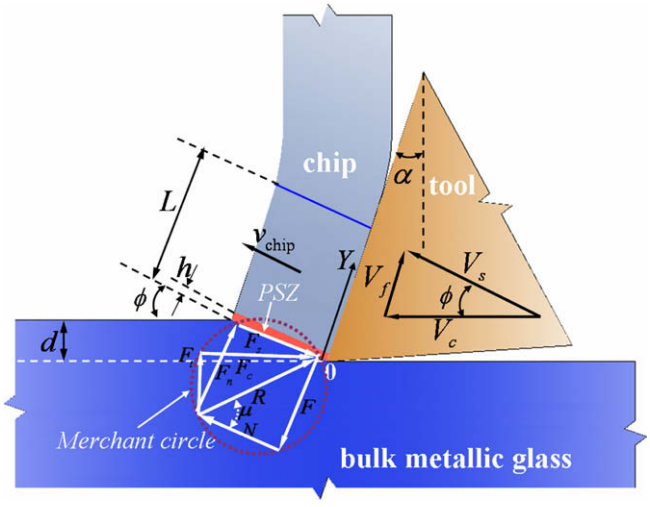

Fig. 5. One-dimensional primary shear zone model of orthogonal cutting.

The dynamic thermomechanical deformation of materials in PSZ can be accurately modeled as a one-dimensional simple shear [21–23,37]. Considering per unit volume of BMG removed, there exists an energy balance [38–40]:

$$W = W_s + W_f + R/d, \tag{1}$$

where $W = F_c/(wd)$ is the total energy expended in cutting, $W_s = F_s V_s/(V_c wd)$ is the shear energy, $W_f = F_c V_f/(V_c wd)$ is the energy expended in friction between chip and tool, and the work R/d of new surface formation ahead of tool tip is involved following Atkins [39,40]; w is the width of chip, d is the depth of cut, the shear force along the PSZ is $F_s = F_c\cos\phi - F_t \sin\phi$ with F_c the cutting force and F_t the thrust force, the cutting velocity V_c, the shear velocity V_s, and the chip velocity V_f satisfy the vector relationship: $\vec{V}_s = \vec{V}_c + \vec{V}_f$, R is the specific work of surface formation. According to the known Merchant Circle (as shown by the asterisk in Fig. 5) [34], we have:

$$\begin{aligned} &\vec{F}_t + \vec{F}_c \equiv \vec{F}_n + \vec{F}_s \equiv \vec{\mathrm{R}}', \\ &\vec{F}_f + \vec{N} \equiv \vec{\mathrm{R}} \equiv -\vec{\mathrm{R}}', \end{aligned} \tag{2}$$

where $\vec{\mathrm{R}}'$ is the force which the workpiece exerts on the chip, F_n is the normal force on the PSZ, and the force $\vec{\mathrm{R}}$ which the tool exerts on the chip can be resolved along the tool face into a friction force F_f and a normal force N. Using Eqs. (1) and (2), now gives an important balance of forces:

$$N = \Gamma(\alpha, \phi, \mu, Z)F_s, \tag{3a}$$

with

$$\Gamma = \Gamma_1 + \Gamma_2 Z, \tag{3b}$$

where $\Gamma_1 = \frac{\cos\mu}{\cos(\mu-\alpha)}\frac{\cos\alpha}{\cos(\phi-\alpha)-\sin\phi}$, $\Gamma_2 = \frac{\sin\phi\cos(\mu-\alpha)}{\cos\mu}\frac{\cos(\phi-\alpha)}{\cos(\phi-\alpha)-\sin\phi}$, and $Z = R/\tau_y d$; μ is the friction angle, τ_y is the shear yield stress. In order to highlight the essential physics, we simplify the geometry by assuming that $\phi = \alpha = 5°$. In this case, $\Gamma_1 \sim 1$ and $\Gamma_2 \sim 0.1$. Furthermore, the present Vit 1 BMG with $\tau_y \sim 1$ GPa is 'no or less' ductile [30,31,41]. If R is considered to be in the 1–10 J m^{-2} range at a rough estimate, Z is about 10^{-2}–10^{-1} in the present machining. Therefore, the term $\Gamma_2 Z$ associated with the surface work is much smaller than the first term Γ_1 and can be neglected in the following calculations. Certainly, it is very interesting and important to determine quantitatively the surface work in the machining of BMGs by using the force intercept method developed by Atkins [39,40], which deserves to be studied in our later work. Following Burns' assumption [22] that the tool is in contact with the workpiece along a constant length L during cutting, the shear stress τ applied homogeneously within the PSZ can be obtained from Eq. (3), which is $\tau = \sigma L\sin\phi/(\Gamma d)$, where σ is the local compressive stress along L and its time differential is proportional to the difference in the V_s and the local velocity v_{chip} of the chips [21,22]. The time differential of τ, therefore, can be expressed as:

$$\frac{d\tau}{dt} = \Lambda(\dot{\gamma}_{avg} - \dot{\gamma}^p), \tag{4}$$

where $\Lambda = ELh\sin^2\phi/\Gamma d^2$ is an apparent shear modulus of the workpiece, with the Young's modulus E, $\dot{\gamma}_{avg} = V_s/h$ is defined as the average strain rate applied the PSZ, and $\dot{\gamma}^p = v_{chip}/h$ is defined as a plastic strain rate in the PSZ. If $\alpha = \phi \to 0$, Eq. (4) can be converted into the result of Burns et al. [22]. In fact, Eq. (4) indicates that the material in the PSZ undergoes an elastic–plastic shearing during cutting. Initially, this shear stress will cause the material in the PSZ to deform elastically. But eventually τ will exceed the yield stress, and plastic flow will take place inside the PSZ in order to dissipate the excess energy. The microscopic mechanism that governs plastic flow in metallic glasses has been discussed by Spaepen [24], Argon [25], etc. The plastic strain rate $\dot{\gamma}^p$ for BMG is given by [18]:

$$\dot{\gamma}^p = 2f\exp\left(-\frac{1}{\xi}\right)\sinh\left[\frac{\tau\Omega}{2k_BT}\right]\exp\left[-\frac{\Delta G_m}{k_BT}\right], \tag{5}$$

where f is the frequency of atomic vibration, ξ is the free volume concentration, Ω is the atomic volume, k_B is the Boltzmann constant, T is the absolute temperature, and ΔG^m is the activation energy.

In order to examine the respective effect of temperature and free volume on the chip formation, we purposely consider two balances about T and ξ in PSZ, i.e.

$$\frac{d\xi}{dt} = \eta(\xi_0 - \xi) + g(\tau, \xi, T), \tag{6}$$

$$\frac{dT}{dt} = \vartheta(T_0 - T) + A\tau\dot{\gamma}^p, \tag{7}$$

where $\eta = (V_f + 4D/h)/h$ is the free-volume flow coefficient with the diffusion coefficient D of ξ, ξ_0 is the free volume concentration outside the PSZ, $g(\tau, \xi, T)$ is the net generation rate function of ξ, and its explicit expression was given by Spaepen [24] and Stief et al. [42], $\vartheta = (V_f + 4\kappa/h)/h$ is the heat flow coefficient with the thermal diffusivity κ, T_0 is the absolute temperature outside the PSZ, $A = \beta_{TQ}/\rho C_v$ is a constant related to the Taylor–Quinney coefficient β_{TQ} with the density ρ and the specific heat C_v. Eqs. (6) and (7) state that the rate of change of free volume concentration ξ or temperature T in PSZ is governed by their respective flow (the first term), including convection and diffusion, and source or creation (the second term); here, we assume for simplicity that either the free volume or heat flow only occurs on the boundary surfaces of the PSZ.

Introducing the dimensionless temperature $\hat{T} = T/T_0$, time $\hat{t} = t/t_0$ with $t_0 = f^{-1}\exp(\Delta G^m/k_BT_0)$, and shear stress $\hat{\tau} = \tau/\tau_0$ with $\tau_0 = 2k_BT_0/\Omega$, then dropping the hats, we have the dimensionless forms of governing Eqs. (4)–(7):

$$\frac{d\tau}{dt} = \Lambda(\dot{\gamma}_{avg} - \dot{\gamma}^p), \tag{8a}$$

$$\dot{\gamma}^p = 2\exp\left[E_A\left(1 - \frac{1}{T}\right)\right]\exp\left(-\frac{1}{\xi}\right)\sinh\left(\frac{\tau}{T}\right), \tag{8b}$$

$$\frac{d\xi}{dt} = \eta(\xi_0 - \xi) + \frac{1}{\varphi}\exp\left[E_A\left(1 - \frac{1}{T}\right)\right]\exp\left(-\frac{1}{\xi}\right) \times \left\{\frac{T}{\Phi\xi}\left[\cosh\left(\frac{\tau}{T}\right) - 1\right] - \frac{1}{n_D}\right\}, \tag{9}$$

$$\frac{dT}{dt} = \vartheta(1 - T) + B\tau\dot{\gamma}^p, \tag{10}$$

where $\Lambda = ELh\sin^2\phi/\Gamma\tau_0 d^2$, $E_A = \Delta G^m/k_BT$, $\eta = (V_f + 4D/h)t_0/h$, φ is a geometrical factor, $\Phi = \frac{2}{3}\frac{1+\nu}{1-\nu}\frac{v^*}{\Omega}\frac{G}{\tau_0}$ with Poisson ratio ν, the critical volume v^* of the effective hard-sphere size of atom, and the shear modulus G, n_D is the number of diffusive jumps necessary to annihilate a free volume equal to v^*, $\vartheta = (V_f + 4\kappa/h)t_0/h$, and $B = A\tau_0/T_0$. Thus, Eqs. (8)–(10) constitute the nonlinear dynamic model for BMG cutting. In addition, very different from the cutting model for serrated chip formation in crystalline metals [21–23,37], the dynamic evolution of free volume is incorporated in our present model. In addition, the contribution of free volume dynamics to plastic flow is taken into account.

4.2. Linear perturbation analysis and limit cycle

In this section, we will reveal the onset criterion for the observed lamellar chip formation in cutting BMGs through a first-order perturbation analysis. Obviously, this coupled thermomechanical cutting model system (8)–(10) displays a rich and complex nonlinear nature; its trajectory (τ, ξ, T) depends very sensitively on the parameters involved. Small differences could trigger vast and often unsuspected results. First, the steady state of the system can easily obtained by $(d\tau^*/dt, d\xi^*/dt, dT^*/dt) = \mathbf{0}$, where

$$\xi^* \approx \frac{\xi_0 + \sqrt{\xi_0^2 + 4\dot{\gamma}_{avg}/\psi\Phi\eta}}{2}, \tag{11}$$

$$\tau^* \approx \ln(\dot{\gamma}_{avg}/2) + \frac{1}{\xi^*}, \tag{12}$$

$$T^* \approx 1 + \frac{B\tau^*\dot{\gamma}_{avg}}{\vartheta}. \tag{13}$$

This describes the homogeneous flow in the PSZ, corresponding to perfect-continuous chip formation during cutting. By linearizing the system (8)–(10) with respect to its steady state (11)–(13) and further exploiting the eigenvalues of the resulting Jacobian matrix, we find that the initiated perturbations will not die out if and only if the free-volume flow coefficient η is greater than a critical value η_c, that is:

$$\eta > \eta_c = \left(\Lambda - \frac{4}{\alpha\Phi\left(\xi_0 + \sqrt{\xi_0^2 + 4\dot{\gamma}_{avg}/\alpha\Phi\eta_c}\right)^3}\right)\dot{\gamma}_{avg}. \tag{14}$$

The inequality indicates that the free-volume flow coefficient is the slaved parameter for the stability of the system of BMG cutting, rather than the heat flow. Note also that the free-volume flow coefficient depends closely on the

material properties and the cutting processes. For example, the effect of the dimensionless cutting speed ($V_c t_0/h$) on η and η_c is shown in Fig. 6a. The region below the red critical curve corresponds to the steady state (11)–(13) of the system. The points within the region between η and η_c correspond to unstable solutions, which will result in lamellar chip formation (see below). As the cutting speed increases, η increases more quickly than η_c, facilitating the instability. The inset in Fig. 6a shows that the instability can occur at relatively low speeds. The region above the η curve is never unattainable if shear localization occurs [35,36]. Fig. 6b shows the variation of η_c with dimensionless cutting depth ($d/\sqrt{Lh}$). It can be seen that η_c decreases (easier instability) with increasing cutting depth. These results are very consistent with the experimental observations [8,17,20].

Since the perturbation analysis is only valid for early time after instability, the system (8)–(10) must be solved numerically for the long-term trajectory. Due to the system's sensitivity, a reasonable estimate of the parameters involved in it should first be performed. Experimental observations indicate that L is of the same order of magnitude as the depth of cut [43], thus $L \approx d = 100$ μm. According to Fig. 3f, h is of the order of micrometers. Considering that Λ is actually the dimensionless shear modulus, we choose $\Lambda \sim 80$ for simplicity. In addition, $\dot{\gamma}_{avg} \sim V_f \sim 10^{-2}$, because $V_c = 0.07\ \mathrm{m\ s^{-1}}$. For the present Vit 1 BMG [41,44,45], $E_A \approx 18.42$, $\nu = 0.36$, $\nu^*/\Omega = 0.8$, $n_D = 3$, $\beta_{TQ} = 0.9$, $\rho = 6125\ \mathrm{kg\ m^{-3}}$, $C_v = 420\ \mathrm{J\ kg^{-1}\ K^{-1}}$, $\xi_0 = 0.05$, $D \sim 10^{-16}\ \mathrm{m\ s^{-2}}$, $\kappa \sim 10^{-6}\ \mathrm{m\ s^{-2}}$. Furthermore, we have $\Phi = 110$, $B = 0.533$. In addition, the free-volume flow coefficient η is estimated to be of the order of 10^{-1}, which depends mainly on its convection, not its diffusion. The heat flow coefficient ϑ, however, is of the order of 10^{1}, and is dominated by its diffusion due to the low cutting speed. Inserting the relevant parameters into the critical condition (14), we obtain the critical free-volume flow coefficient $\eta_c \sim 0.2$–0.3 for instability.

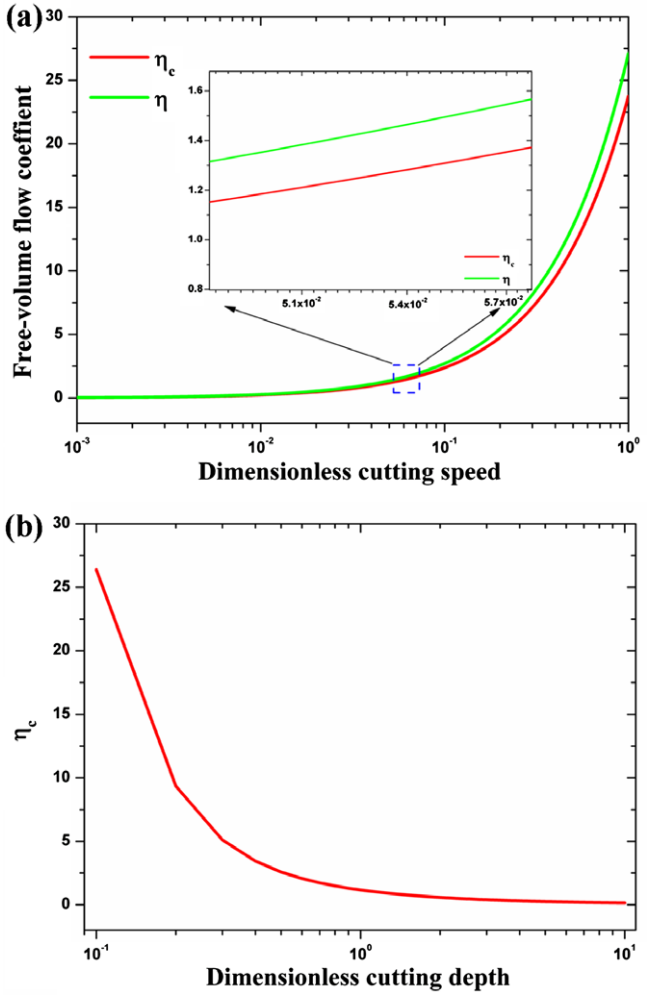

Fig. 6. (a) Effects of dimensionless cutting speed on the free-volume flow coefficient and its critical value. (b) Effects of dimensionless cutting depth on the critical free-volume flow coefficient.

For a fixed $\eta = 0.1 < \eta_c$, the shear stress τ, the free volume concentration ξ, and the temperature T vs. the cutting time t with $\vartheta = 0.4$, 4.0 and 40 is shown in Fig. 7a–c, respectively. Their trajectories (τ, ξ, T) finally reach three limit points, as shown in Fig. 7d. It is found that even if the heat flow coefficient (10^{-1}) is two orders of magnitude lower than that (10^{1}) of conventional metal, the perturbation will immediately die out if and only if the free-volume flow coefficient is lower than its critical value. This implies that the thermal instability is not the controlling factor for the stability of the system of BMG cutting. On the other hand, once $\eta = 0.4 > \eta_c$, the system becomes unstable. Its trajectory (τ, ξ, T) with $\vartheta = 0.4$, 4.0 and 40 is shown in Fig. 8a–c, respectively. In this case, the shear stress τ, the free volume concentration ξ, and the temperature T display a self-sustained periodic oscillation towards stable limit cycles (Fig. 8d), regardless of the heat flow coefficient. The stable limit cycles correspond to the formation of periodic lamellar chips. Also, we note that increasing the heat flow coefficient from Fig. 8a–c decreases the oscillation amplitude and period of the limit cycle. This means that the thermal instability only affects the shape of a lamellar chip, such as amplitude or spacing, not its onset. Fig. 8c satisfactorily corresponds to our present machining case. We find there is no appreciable rise in the temperature (see Fig. 8c inset), yet the limit cycle instability still takes place. The stable oscillation periodic t is about 10 (or 10^{-4} s), corresponding to the spatial spacing $\delta^c = V_f t \sim$ μm. This value agrees very closely with the actual measured value of spacing of lamellar chip (see Fig. 1c and f). Therefore, one can conclude that the lamellar chip formation in BMG cutting is dominated by the dynamic instability of free volume flow and source, whereas the thermal instability only plays a role in the morphology of lamellar chips.

4.3. Lamellar chip formation

Our theoretical simulations, together with the experimental observations, provide us with an insight into the physical picture of lamellar chip formation during BMG

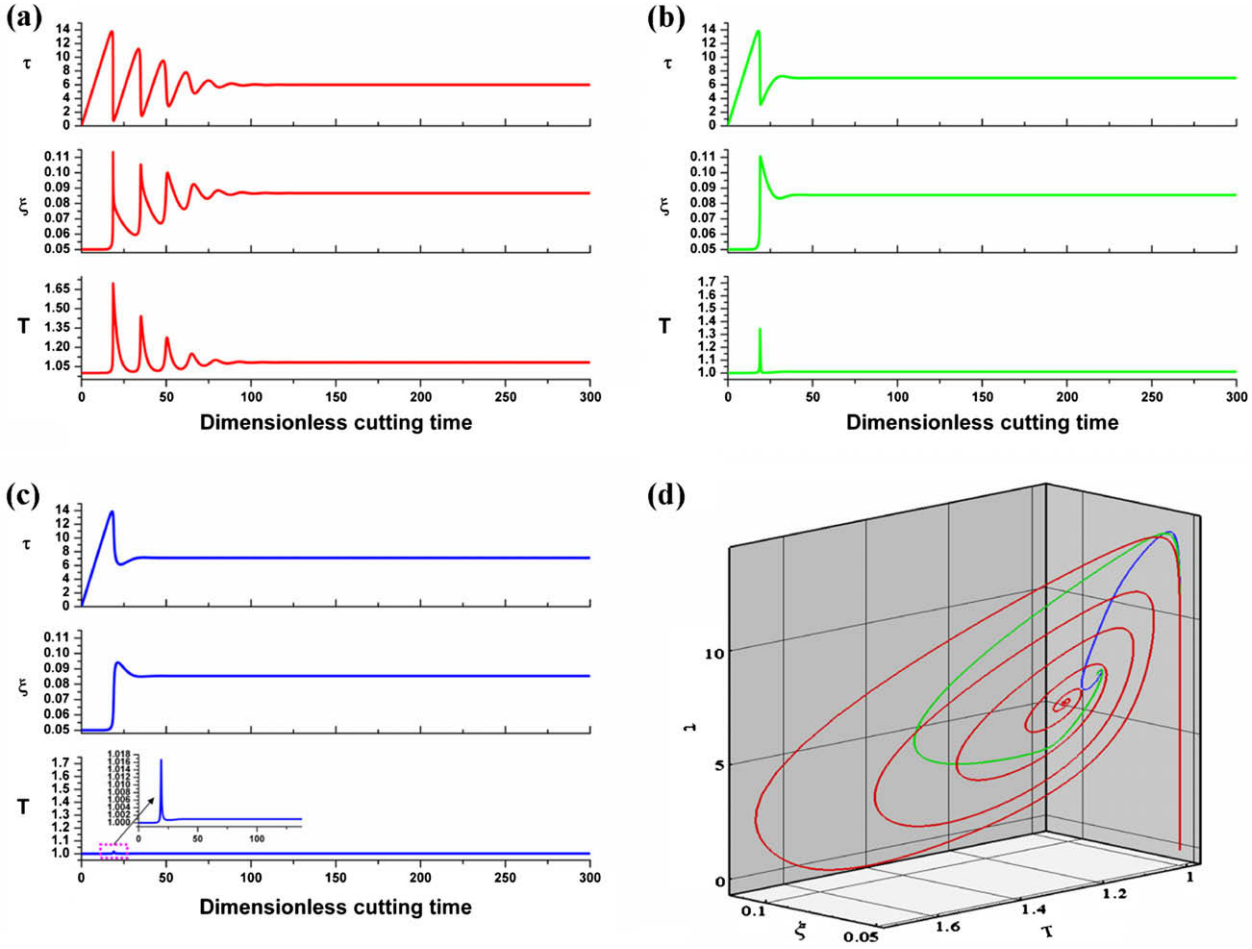

Fig. 7. Shear stress τ, free volume concentration ξ, and temperature T vs. time t from simulations of Eqs. (8)–(10) with (a) $\vartheta = 0.4$, (b) $\vartheta = 4.0$ and (c) $\vartheta = 40$ and fixed $\eta = 0.1$. (d) Trajectories (τ, ξ, T) converging towards stable limit points.

cutting as well as the differences in the mechanism involved compared with conventional serrated chips. During BMG cutting processes, the BMG, entering the PSZ, initially deforms elastically because of relatively low applied shear stress. With the continuous increase in stress, the source of free volume concentration exceeds its flow, finally leading to a drastic creation in free volume. The net increase in free volume, in turn, results in a catastrophic drop in shear stress. If its flow, eventually, balances its source, a steady-state free volume is achieved at which the shear stress stays constant. Then, a homogeneous plastic flow occurs in the PSZ, where a steady-state temperature field is also reached due to the conversion of plastic work into heat. The constant shear stress, free volume concentration and temperature in the PSZ indicate a stable state (see Fig. 7), i.e. a limit point of the system. In this case, the workpiece is cut via uniform plastic flow occurring in the PSZ, implying a perfect-continuous chip. However, the flow in BMGs is prone to localization into very thin shear bands if the source rate of free volume is faster than its flow (creation) rate [35,36]. The initiation and propagation of a shear band will decrease the shear stress within the PSZ due to energy dissipation. The shear stress unloading to the elastic range slows down the free volume source, whereas the material moving outwards in the PSZ speeds up the free volume flow. This brings about a decrease in the free volume concentration. At the same time, the heat production also ceases, and the heat flow cools the PSZ. Soon, enough new material passes through the PSZ to increase the shear stress again. A consequence is that the free volume concentration and the temperature build up again; thus the cutting cycle repeats itself. As we have shown previously (Fig. 8), this provides the autonomous feedback in shear stress, free volume and temperature which leads to self-sustained periodic oscillations in these fields inside the PSZ. The periodic motion resulting from repeated shear-band formation describes the periodic lamellar chip formation. Now, we realize that, although both types of chip originate from the repeated shear localization, the lamellar chip and the serrated chip have distinct physical mechanisms. In BMG cutting, the lamellar chip forms due to the breaking of static equilibrium of the free volume flow and source. In conventional metal cutting, however, the serrated chip formation results from the breaking of the static equilibrium of the heat flow and source.

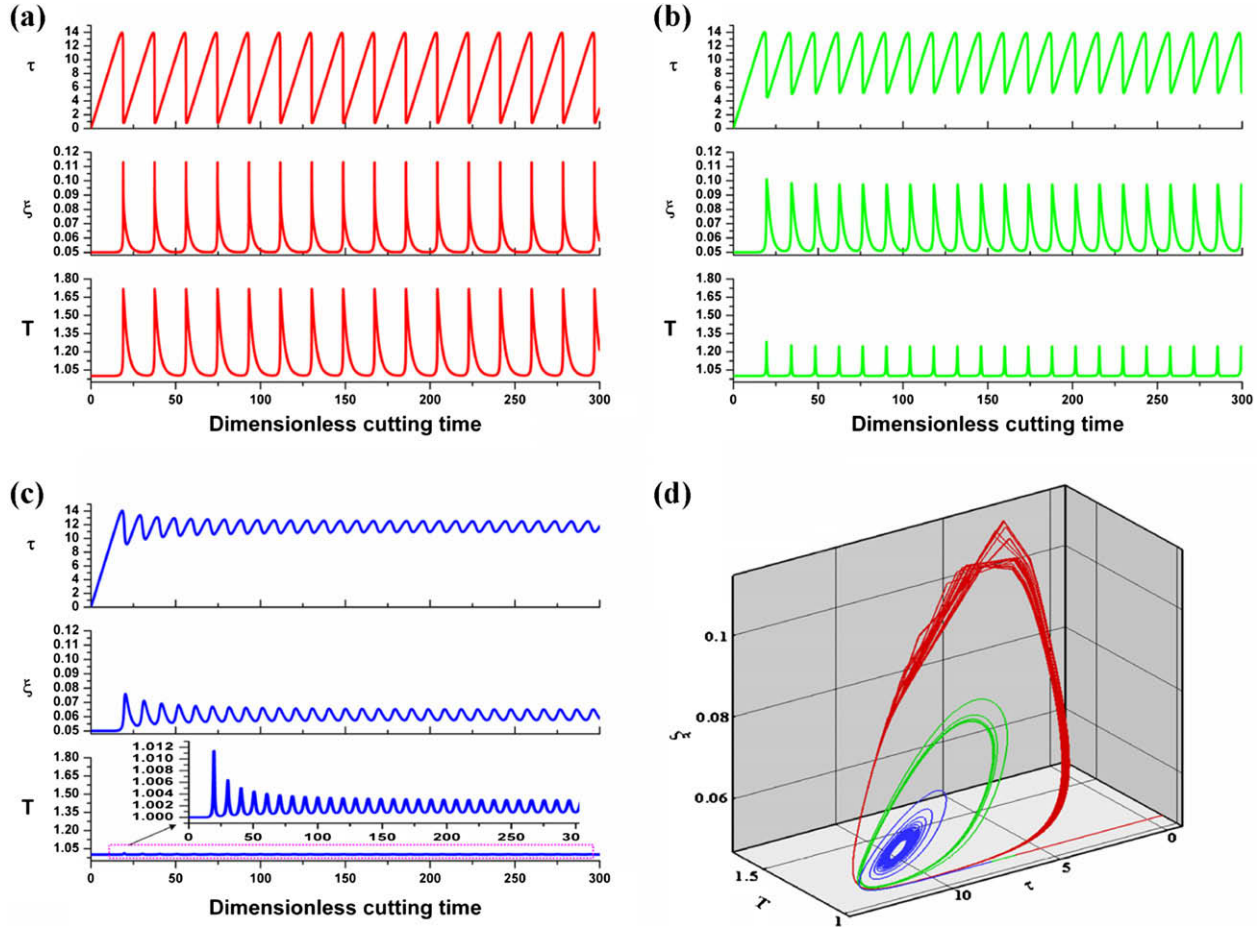

Fig. 8. Shear stress τ, free volume concentration ξ, and temperature T vs. time t from simulations of Eqs. Eqs. (8)–(10) with (a) $\vartheta = 0.4$, (b) $\vartheta = 4.0$ and (c) $\vartheta = 40$ and fixed $\eta = 0.4$. (d) Trajectories (τ, ξ, T) converging towards stable limit cycles.

5. Concluding remarks

In summary, cutting BMGs, even at low speeds, usually produces "continuous" chips characterized by lamellae. We present a nonlinear dynamic model, taking into account the autonomous feedback among stress, free volume and temperature, to reveal the mechanism underlying these chips. The symmetry breaking of free volume flow and source governs the onset of lamellar chips, while the thermal instability only affects their morphology. Mathematically, lamellar chip formation can be understood as the manifestation of a self-sustained stable limit-cycle bifurcation phenomenon. Our results provide some important clues for BMG cutting techniques. Increasing the cutting speed V_c and the depth of cut d will tend to produce lamellar chips. Under the same conditions, those BMGs with higher initial free volume concentration and larger Poisson ratio or shear modulus, decreasing the η_c (see Eq. (14)), will have a decreased likelihood of forming lamellar chips. Decreasing the heat flow coefficient will facilitate viscous flow, favoring chips becoming more lamellar. In conventional metal cutting, we must focus our mind on the thermal instability. In addition to thermal instability, however, specific attention is paid to the stress-driven free volume instability during BMG cutting.

Acknowledgments

This work has been supported by the Natural Science Foundation of China (Grants Nos. 10725211, 10721202), the National Basic Research Program of China (Grant No. 2009CB724401), and the Key Project of Chinese Academy of Sciences (Nos. KJCX2-YW-M04 and KJCX-SW-L08).

References

[1] Trent EM, Wright PK. Metal cutting. forth ed. BH Publications; 2000. p. 339.
[2] Gente A, Hoffmesiter HW, Evans CJ. Chip Formation in Machining Ti6Al4V at Extremely High Cutting Speeds. CIRP Ann 2001;50:49.
[3] Ernst H, Martellotti M. The formation of the built-up edge. ASME Mech Eng 1938;57:487.
[4] Vyas A, Shaw MC. Mechanics of saw-tooth chip formation in metal cutting. J Manuf Sci Eng 1999;121:163.
[5] Rice WC. The formation of continuous chips in metal cutting. Eng J Eng Inst Can 1961;44:41.
[6] Recht RF. Catastrophic thermoplastic shear. ASME J Appl Mech 1964;31:189.

[7] Findley WN, Reed RM. The influence of extreme speeds and rake angles in metal cutting. ASME J Eng Ind 1963;85:49.
[8] Bakkal M, Shih AJ, Scattergood RO. Chip formation, cutting forces, and tool wear in turning of Zr-based bulk metallic glass. Int J Mach Tools Manuf 2004;44:915.
[9] Komanduri R, Merchant ME, Shaw MC. US machining and grinding research in the 20th century. Appl Mech Rev 1993;46:70.
[10] Johnson WL. Bulk glass-forming metallic alloys: science and technology. Mater Res Soc Bull 1999;24:42.
[11] Inoue A. Stabilization of metallic supercooled liquid and bulk amorphous alloys. Acta Mater 2000;48:279.
[12] Wang WH, Dong C, Shek CH. Bulk metallic glasses. Mater Sci Eng R 2004;44:45.
[13] Ashby MF, Greer AL. Metallic glasses as structural materials. Scripta Mater 2006;54:321.
[14] Schuh CA, Hufnagel TC, Ramamurty U. Mechanical behavior of amorphous alloys. Acta Mater 2007;55:4067.
[15] Eckert J, Das J. Mechanical properties of bulk metallic glasses and composites. J Mater Res 2007;22:285.
[16] Dai LH, Bai YL. Basic mechanical behaviors and mechanics of shear banding in BMGs. Int J Impact Eng 2008;34:704.
[17] Bakkal M, Shih AJ, Scattergood RO, Liu CT. Machining of a Zr-Ti-Al-Cu-Ni metallic glass. Scripta Mater 2004;50:583.
[18] Bakkal M, Shih AJ, McSpadden SB, Liu CT, Scattergood RO. Light emission, chip morphology, and burr formation in drilling the bulk metallic glass. Int J Mach Tools Manuf 2005;45:741.
[19] Chen XH, Zhang XC, Zhang Y, Chen GL. Fabrication and characterization of metallic glasses with a specific microstructure for micro-electro-mechanical system applications. J Non-Cryst Solids 2008;354:3308.
[20] Ueda K, Manabe K. Chip formation mechanism in microcutting of an amorphous metal. CIRP Ann 1992;41:129.
[21] Burns TJ, Davies MA. On repeated adiabatic shear band formation during high-speed machining. Int J Plastic 2002;18:487.
[22] Burns TJ. Nonlinear dynamics model for chip segmentation in machining. Phys Rev Lett 1997;79:447.
[23] Palmai Z. Chaotic phenomena induced by the fast plastic deformation of metals during cutting. Trans ASME 2006;73:240.
[24] Spaepen F. A microscopic mechanism for steady state inhomogeneous flow in metallic glasses. Acta Metall 1977;25:407.
[25] Argon AS. Plastic deformation in metallic glasses. Acta Metall 1979;27:47.
[26] Spaepen F. Physics of defects. Amsterdam: North-Holland; 1981. p. 153.
[27] Peker A, Johnson WL. A highly processable metallic glass: Zr-Ti-Cu-Ni-Be. Appl Phys Lett 1993;63:2342.
[28] Inoue A. High strength bulk amorphous alloys with low critical cooling rates. Mater Trans JIM 1995;36:866.
[29] Johnson WL. Curr Opin Solid State Mater Sci 1996;1:383.
[30] Zhang ZF, Eckert J, Schultz L. Difference in compressive and tensile fracture mechanisms of $Zr_{59}Cu_{20}Al_{10}Ni_3Ti_3$ bulk metallic glass. Acta Mater 2003;51:1167.
[31] Jiang MQ, Ling Z, Meng JX, Dai LH. Energy dissipation in fracture of bulk metallic glasses via inherent competition between local softening and quasi-cleavage. Philos Mag 2008;88:407.
[32] Wang G, Chan KC, Xu XH, Wang WH. Instability of crack propagation in brittle bulk metallic glass. Acta Mater 2008;56:5845.
[33] Argon AS, Salama M. The mechanism of fracture in glassy materials capable of some inelastic deformation. Mater Sci Eng 1976;23:219.
[34] Merchant ME. Mechanics of the metal cutting process. I. Orthogonal cutting and a type 2 chip. J Appl Phys 1945;16:267.
[35] Dai LH, Yan M, Liu LF, Bai YL. Adiabatic shear banding instability in bulk metallic glasses. Appl Phys Lett 2005;87:141916.
[36] Jiang MQ, Dai LH. On the origin of shear banding instability in metallic glasses. Unpublished work; 2009.
[37] Xie JQ, Bayoumi AE, Zbib HM. Analytical and experimental study of shear localization in chip formation in orthogonal machining. J Mater Eng Perform 1995;4:32.
[38] Merchant ME. Basic Mechanics of the Metal Cutting Process. Trans ASME 1944;66:A65.
[39] Atkins AG. Modelling metal cutting using modern ductile fracture mechanics: quantitative explanations for some longstanding problems. Int J Mech Sci 2003;45:373.
[40] Atkins AG. Toughness and cutting: a new way of simultaneously determining ductile fracture toughness and strength. Eng Fract Mech 2005;72:849.
[41] Liu LF, Dai LH, Bai YL, Wei BC. Initiation and propagation of shear bands in Zr-based bulk metallic glass under quasi-static and dynamic shear loadings. J Non-Cryst Solids 2005;351:3259.
[42] Stief PS, Spaepen F, Hutchinson JW. Strain localization in amorphous metals. Acta Metall 1982;30:447.
[43] Shaw MC. Metal cutting principles. Oxford: Oxford University Press; 1984.
[44] Lewandowski JJ, Greer AL. Temperature rise at shear bands in metallic glasses. Nature Mater 2006;5:15.
[45] Gao YF, Yang B, Nieh TG. Thermomechanical instability analysis of inhomogeneous deformation in amorphous alloys. Acta Mater 2007;55:2319.